Analyzing data from the single dot spectroscopy of silicon quantum dots

Nathanyel Schut
Dirk Kuiper

February 1, 2021

Abstract

Silicon nanoparticles are of great interest to many industries as they have a size tunable bandgap, which gives them many different applications. In this study characteristics of these nanoparticles are studied and analyzed by writing a program which makes raw data from single dot spectroscopy easy to interpret. The final goal of this study is to create a visual representation of two main characteristics of the quantum dots: the FWHM (full width at half maximum) and the central energy of the detected quantum dots. These two values were found to be respectively 0.20 and 1.7 eV on average.

STUDENTNUMBERS	12907995 (Nathanyel) & 12416657 (Dirk)
EVALUATOR	Dr. Ankit Goyal PhD
COURSE	Research practicum
ASSIGNMENT	Research report
VERSION	Final version
BACHELOR	Physics- & Astronomy year 2

VU VRIJE UNIVERSITEIT AMSTERDAM | UNIVERSITEIT VAN AMSTERDAM

Contents

1 Introduction

Quantum dots are nanoparticles with a radius smaller than the excitonic Bohr radius [1]. As a consequence, they have a size-tunable band gap energy and thus size-tunable emission energy, which makes them very interesting to study, because this property has many applications multiple work fields, such as: LED's, photovoltaics and biomedical engineering [2].

More specifically silicon nanoparticles (Si-NPs) are an important topic of study and they are the type of semiconductors that will be discussed in this article. Bulk silicon has an indirect band gap, making its emission poor and thus its use in photonics less attractive. However, this property is reduced in Si-NPs due to the quantum confinement effect [1] [3].

Now a common problem in nanomaterials, is that they are often polluting and potentially toxic. These characteristics are often known to have adverse effects on organisms and the environment [4]. Silicon however is an abundant and non-toxic element, which makes it a very promising material for the study and applications of nanomaterials [5].

In this work we analyze the emission spectra of single Si-NPs. More specifically we look at the full width at half maximum (FWHM) of the gaussian curve which models the emission of the single Si-NPs. Additionally, the central energy of this gaussian curve will be analyzed.

2 Theory

The Si-NPs having these electronic and optical properties has everything to do with quantum confinement. The quantum confinement effects can be observed when the diameter of the particle is of the same order of magnitude as the wavelength of the electron wave function [6]. More specifically the confinement of an electron and hole in nanocrystals significantly depends on the material properties, namely, on the Bohr radius a_B [7]. For Si-NPs the exciton Bohr radius has a size of the order of 5 nm [8]. As the confinement becomes smaller and reaches nanoscale, the energy spectrum becomes discrete. Consequentially, the bandgap energy becomes size-dependent. This results in a blueshift in PV emission as the size of the particles decreases [9].

3 Setup and Methodology

3.1 Setup

Correlative microscopy (CM) was used for the spectral analysis of the Si-NPs. This is a technique where both an atomic force microscope (AFM) and a spectrometer are used on the same sample. The AFM acquires depth information on the sample and thus the size of the nanoparticles. The spectrometer contains a charge coupled device (CCD) detector which measures the photoluminescence (PL) of the sample. The CCD consists of 1340 x 400 pixels. Furthermore, the spectrometer contains a mirror and multiple gratings which are interchangeable giving either a PL microscopy image or a PL spectrum. The latter being of interest in this research. The CM-setup also contains a laser in order to excite the Si-NP sample. The correlative microscopy setup is shown in Figure 1.

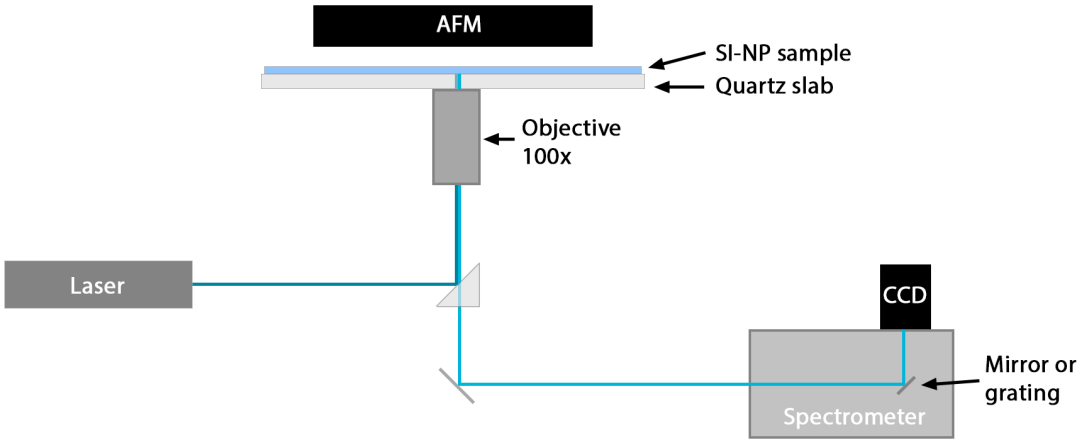

Figure 1: Schematic representation of the correlative microscopy setup used for this research. The atomic force microscope scans the sample from above, while a continuous wave laser excites the sample from below. The emitted photons will eventually enter the spectrometer which may contain a mirror or a grating. Finally, the light will reach the charge coupled device where either a PL-image or a PL-spectrum will be produced.

The PL-image now contains all the Si-NPs in a certain area, and thus the CCD measures the PL-spectrum of all the visible Si-NPs. To obtain spectra of individual Si-NP's, a slit of 1 to a few pixels is taken of the PL-image for which the spectrum is to be analyzed. For each pixel along the slit (the slit is 400 pixels long) the CCD will measure a PL-spectrum, thus if the slit contains a nanoparticle it will measure its spectrum.

3.2 Sample

The Si-NPs were prepared by a PHD-student in Canada. The nanoparticles consist of a crystalline silicon core with an amorphous silicon shell capped with carbon ligands. The Si-NP sample was diluted in hexane and was spread on a 150 μm thick quartz slab of 1 inch diameter. 7 mL of sample was used for the measurements. Finally, the sample was excited at a wavelength of 488 nm (cyan color) by a continuous wave laser.

3.3 Data-Analysis

The acquired data consists of a list of wavelengths (the CCD can measure 1340 different wavelengths) with a corresponding measured intensity for each pixel along the slit. In this case the pixels of the CCD were binned together, since the emission of Si-NPs is too weak to analyze without binning in the time frames that this data was recorded. Because of this, the resolution was reduced from 1340 x 400 pixels to 167 x 200 pixels. All of the data analysis was done with Python 3 programming.

Firstly, the data was corrected for any optical disturbances of the emitted light from the nanoparticles and for the sensitivity of the spectrometer at higher wavelengths. For the correction the emission spectrum of a tungsten lamp was measured the same way as that of the Si-NPs. The tungsten lamp is a black-body radiator and so it's real emission spectrum can be calculated with Planck's Law [10]. Using the measured and calculated spectrum of the tungsten lamp and the measured spectrum of the Si-NP sample, the real spectrum of the nanoparticles can be calculated by

$$I_{RS} = I_{MS} \cdot \frac{I_{RL}}{I_{ML}}, \tag{1}$$

where I_{RS} is the real intensity of the sample at a certain wavelength, I_{MS} is the measured intensity of the sample at that wavelength, I_{RL} is the real intensity of the tungsten lamp and I_{ML} is the measured intensity of the tungsten lamp.

After the correction of the data, the background light was reduced by subtracting the spectrum at a certain slit position from the next slit position (for example: the spectrum at the 399th pixel along the slit was subtracted from the spectrum at the 400th pixel). This corrected data can be represented in a 2-dimensional map as shown in the Results section in Figure 3. The position along the slit is shown on the vertical axis, the energy corresponding to the measured wavelength on the horizontal axis and the colormap shows the corrected intensity.

In some cases, the measurements with the CCD detector were influenced by solar flares. The solar flares showed up as very sharp intensity peaks on a single pixel for a single wavelength on the CCD. These solar flares had to be filtered out, which was done by setting an

intensity threshold. All intensity values above this threshold were set to zero.

The Si-NPs can now be located, since the intensity values of their spectra are significantly higher than a spectrum of an empty spot in the PL-image. By looking at the total intensities (summing over the intensity of each wavelength) of all the pixels along the slit, the positions of the nanoparticles can be localized and thus their spectra can be found. Total intensities above the mean total intensity plus three times the standard deviation were counted as Si-NPs. To prevent taking adjacent spectra with a total intensity above the 3σ threshold as two separate Si-NPs, the script takes the pixel with the highest total intensity as the position of the Si-NP. A plot of the total intensities for a single data-set is shown in Figure 2.

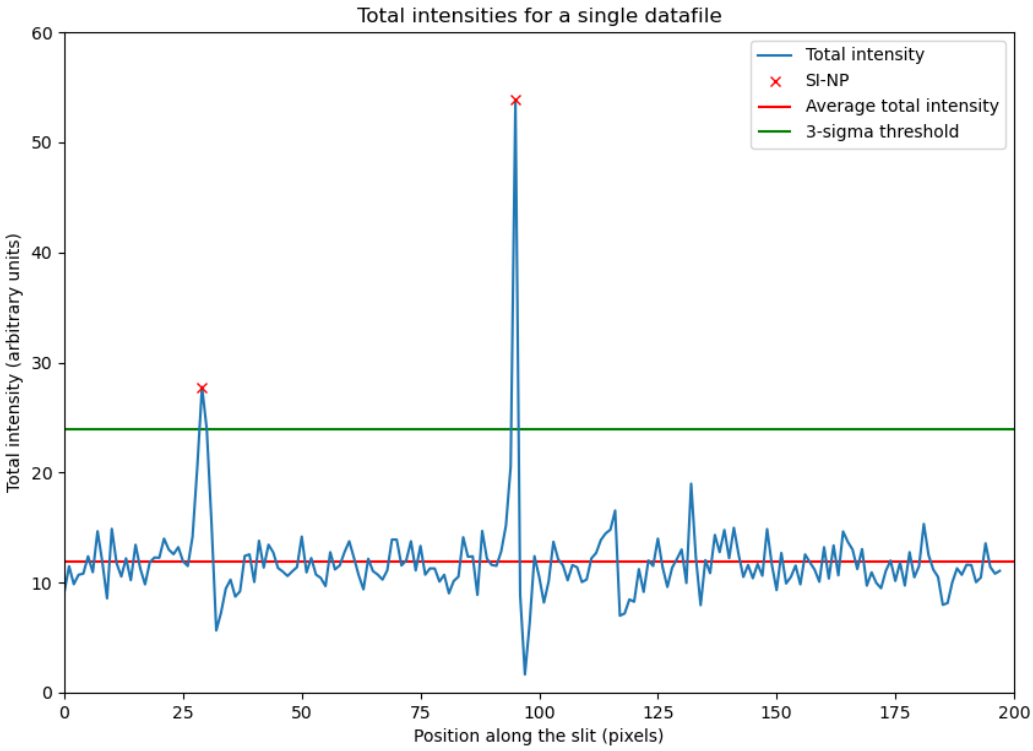

Figure 2: A plot of the total measured intensities per pixel for a single data-set. Binning of pixels was done to increase intensity, so the x-axis counts 200 pixels. The red line in the plot represents the average total intensity, while the green line shows the 3σ threshold. The red crosses indicate the position and total intensity of the Si-NP emission. This slit of the PL-image contains two Si-NPs.

Now that the spectra of the individual Si-NPs are obtained, they can be fitted to a Gaussian curve with one or two peaks. The FWHM and the central energy of this Gaussian curve are of interest in this research, since it gives useful information about the size dependency of the nanoparticles. These properties can be represented in a histogram as shown under the Results section in Figure 5.

4 Results

The Python script for data-analyzing in this research returns 4 two-dimensional maps of both raw and processed data (one map for raw data, one for corrected data without noise reduction, etc.) as shown in Figure 3. Additionally, the script returns the PL-spectra of the nanoparticles found in the selected data-file, with the optimal fit shown in the same plot, all of which is shown in Figure 4. Finally, the script returns a histogram of the FWHM and central energies of the nanoparticles found in all the uploaded files. The histograms can be seen in Figure 5. After leaving out strongly deviating values to properly show the useful data, a Gaussian fit can be done to the data. The fit for the FWHM values gives an average FWHM of 0.2146 ± 0.0034 eV. The fit for the central energy gives an average value of 1.668 ± 0.011 eV. More information about the usage of the script can be found in appendix A.

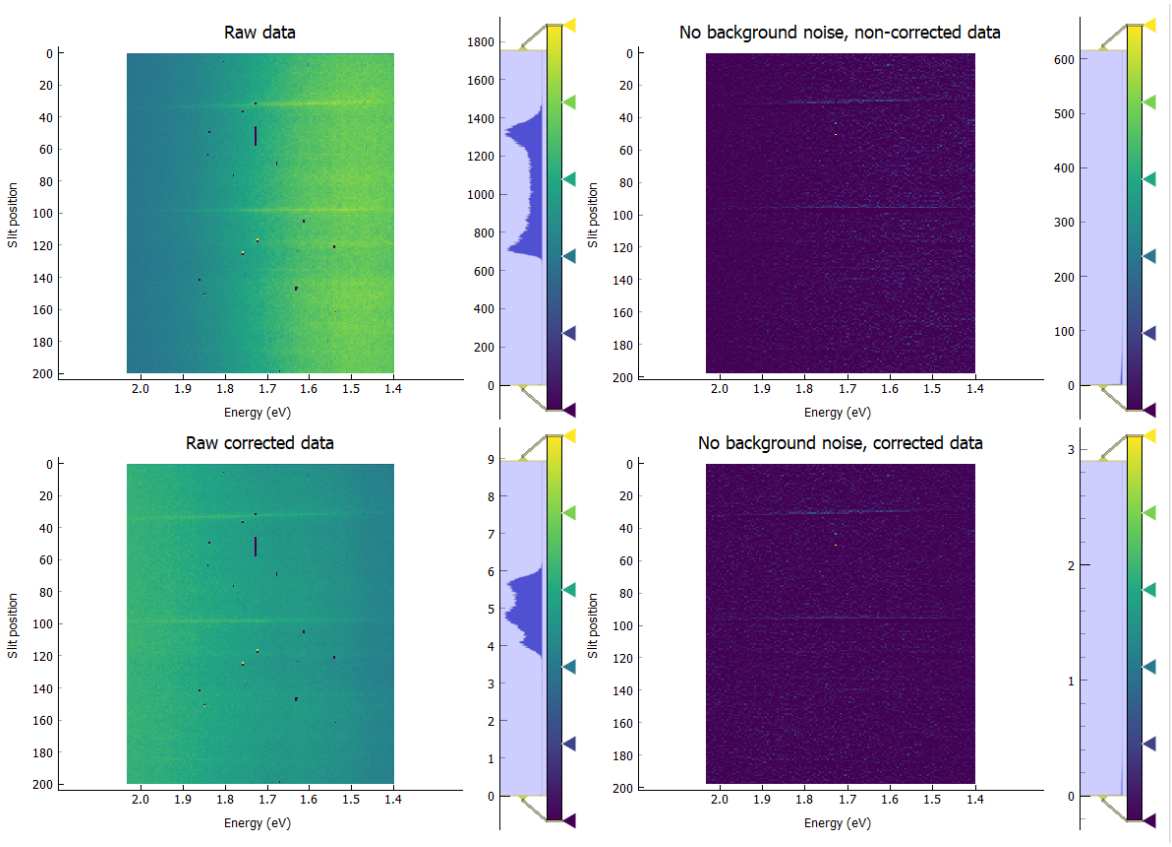

Figure 3: Two dimensional maps of the raw and processed data. The columns separate the data with and without background noise reduction, while the rows separate the data with and without correction. For each map, the energy is plotted on the horizontal axis, while the pixel number along the slit is plotted on the vertical axis.

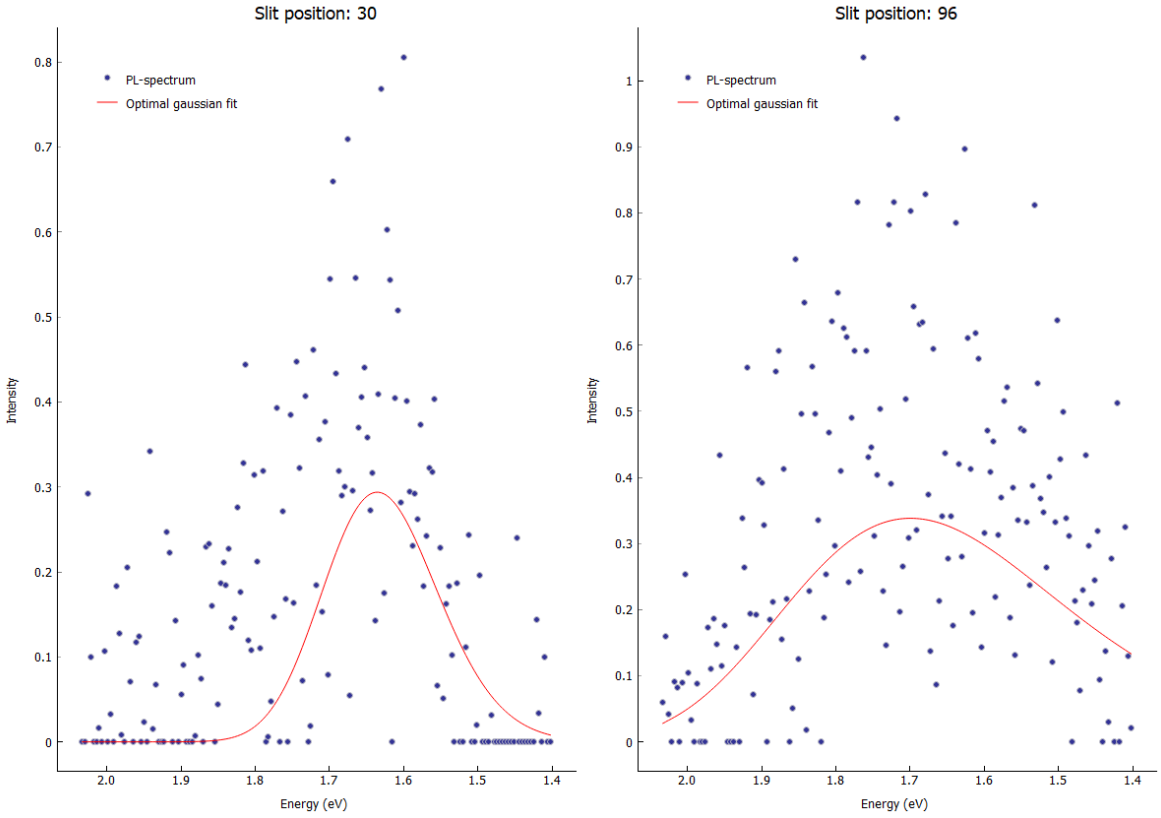

Figure 4: PL-spectra of the nanoparticles found in the data of Figure 3. The blue dots show the measured PL-spectrum and the red line shows the optimal fit of a Gaussian model to this data. The blue dots do not seem to follow the red curve very nicely since the spread of the data is quite large. Because of this, fitting any model would prove rather difficult.

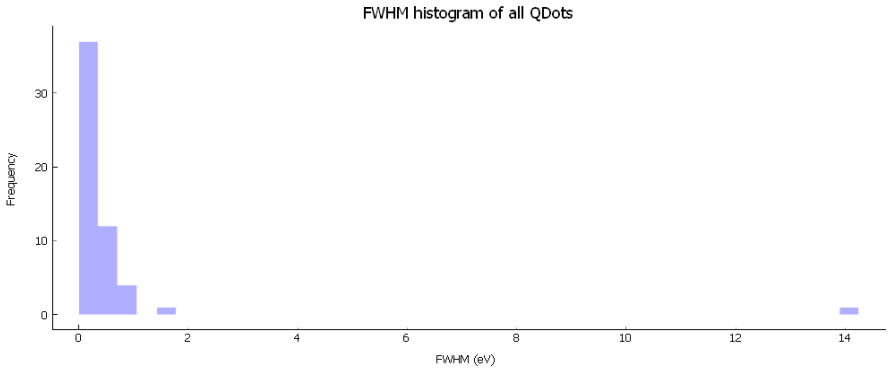

(a) Histogram of FWHM values of all the nanoparticle emission spectra.

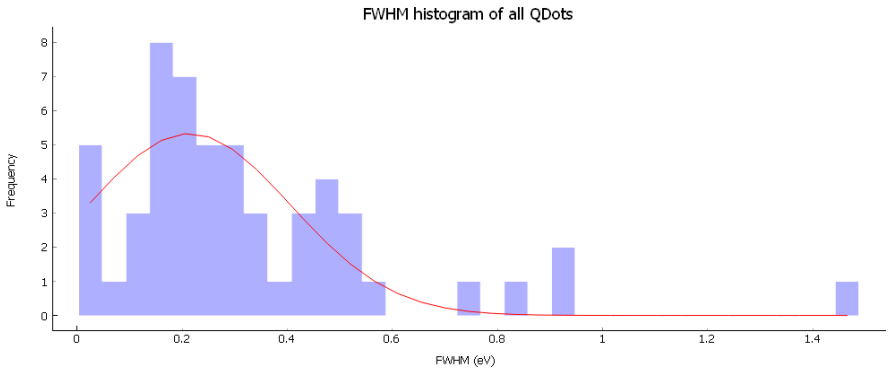

(b) Histogram of FWHM values of a selected group of nanoparticle emission spectra.

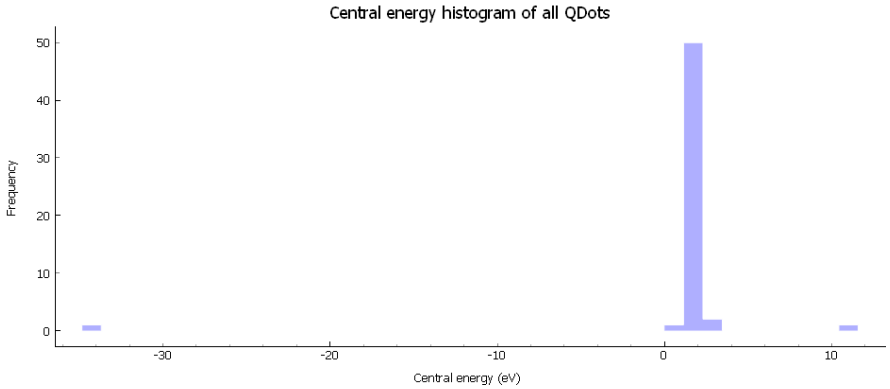

(c) Histogram of central energy values of all the nanoparticle emission spectra.

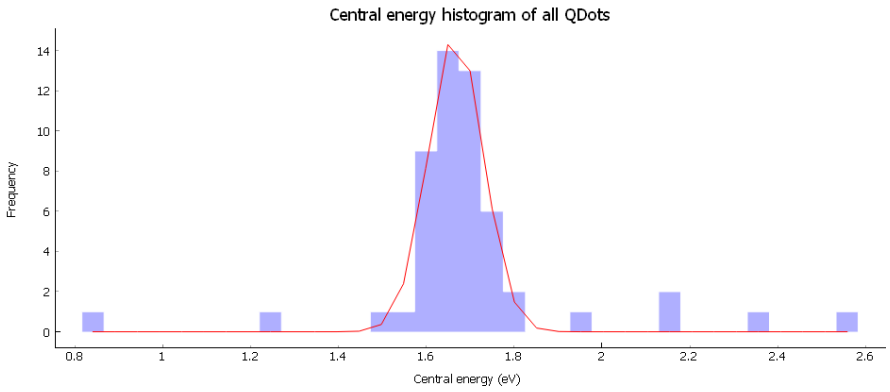

(d) Histogram of central energy values of a selected group of nanoparticle emission spectra.

Figure 5: Histograms for FWHM and central energy of fitted Gaussian curve to the PL-spectra of all Si-NPs and of a selected group of Si-NPs. In (a) the value at around 14 eV deviates strongly from the rest of the FWHM values. This is because some gaussian curves describe the PL-spectrum of a Si-NP very poorly, resulting in strange FWHM and central energy values. (b) shows the same histogram, but without the value at around 14 eV to more clearly see the distribution of FWHM values around the mean. A gaussian curve was fitted to this data with a center at 0.2146 ± 0.0034 eV. Other deviating values of the mean can be seen in (c), for the same reason as (a). These inaccurate values are left out in (d). A gaussian fit to this data gives a mean central energy of about 1.668 ± 0.011 eV.

5 Discussion

5.1 Limitations of the measurements

There are certain factors in the way that data was obtained that had a negative impact on the ability to analyze the given data. For example, most of the data was very noisy, which made it significantly harder to fit a proper Gaussian to the peaks. There were also quite a few peaks in emission, that might have been identified as quantum dots, had there been a longer measuring time. Measuring for a longer time would also have had a positive effect on the noisiness of the data. Another factor that would be worth looking at is the binning that was done by analyzing the data. Binning the data has a positive influence on the noisiness of the data, however it also reduces the resolution of the CCD, which might make for less accurate measurements.

5.2 Limitations of the data analyzing program

The program has an important limiting factor in the fitting that is done after a quantum dot is detected. In the rare case that there would be three or more quantum dots detected in the same line, the program is as of now not able to analyze all dots, it will fit only up to two detected dots in one spectrum. Furthermore, because of the way background noise was reduced, in the case that there would be a quantum dot present in the first slit, it would not be detected. These are both obstacles that can be overcome by visual inspection of the data and graphs, but they are features that would have been great additions to the program had there been more time to work on the script. Another flaw in the analyzing of the data is the removal of solar flares. Currently the script sets all values above a certain threshold to zero, however this threshold is specific for only a few data-sets and might cause a part of the PL-spectrum of a quantum dot to be removed. By creating a detection system for single pixels having higher intensities, this can be prevented. Finally, another great addition that would have only been possible if there had been more time, is the implementation of threads, to reduce the waiting time. As of now the program analyzes all the selected data files and doesn't show any results until the complete analysis is finished. Implementing threads would significantly reduce waiting time and make the interface more user friendly.

5.3 Interpretation of the results

The results of this research tell us that the average band-gap energy is 1.668 ± 0.011 eV. It is hard to tell if this value is in agreement with literature, since we don't know the size distribution of the Si-NPs. According to Huang et al. the band gap energy of these Si-NPs would converge to the band gap energy of bulk silicon for larger Si-NPs. Bulk silicon has a

band gap energy of 1.59 eV, so this would mean that the Si-NPs in this experiment are medium to large in size, since their average band gap energy gets close to that of large Si-NPs. Data of the atomic force microscope in 1 would have to be analyzed to check if the results of this research are in line with literature.

Another factor that should be noted is that only a total of 54 quantum dots were analyzed in Figure 5b. To make the results more reliable, more data files need to be analyzed. However, we currently don't possess these data files.

6 Conclusion

6.1 Script/Program

Overall, the program does a good job of analyzing the given data. It is relatively user friendly and despite the previously named limitations, it provides the user with a good way to get information from the raw measurements. All in all, the goal of writing a script that could call on the data files and analyze them has been accomplished, while even exceeding those expectations, by creating a graphical user interface for easy user interaction. However, there certainly are some implementations that would significantly better the program, had there been more time to work on it. Implementing threads and creating a better filter for measured solar flares for example would significantly increase the efficiency and accuracy of the program. Lastly creating more UI (user interface) elements would further enhance our programs ability to be worked by anyone, even people without any understanding of coding and would also better the compatibility with the datafiles.

6.2 Results

Ultimately, from the given data that was analyzed we found that the average FWHM of the quantum dots was found to be 0.20 eV and the central energy was 1.7 eV. It is hard to make conclusions from these findings, as there is no literature available to compare with at the current moment. To get more results out of the created program more data would have to be analyzed as to make better conclusions for what the findings actually mean.

A Additional information on the script

The script provides a graphical user interface, containing the figures (only two histograms are given, which can be altered to the users liking) in the Results section nested in tabbed windows. The tabbed windows contain the figures for just one data-file and the user has the ability to select the file for which to show the figures after uploading as many files as the user likes. Before uploading the data-files, a correction file has to be uploaded containing the measured intensity values for the tungsten lamp. Currently, there is no user interface for setting the central wavelength of the spectra. The calculation of the wavelengths is specific for the data-files used in this research. This user interface feature will be added in the near future.

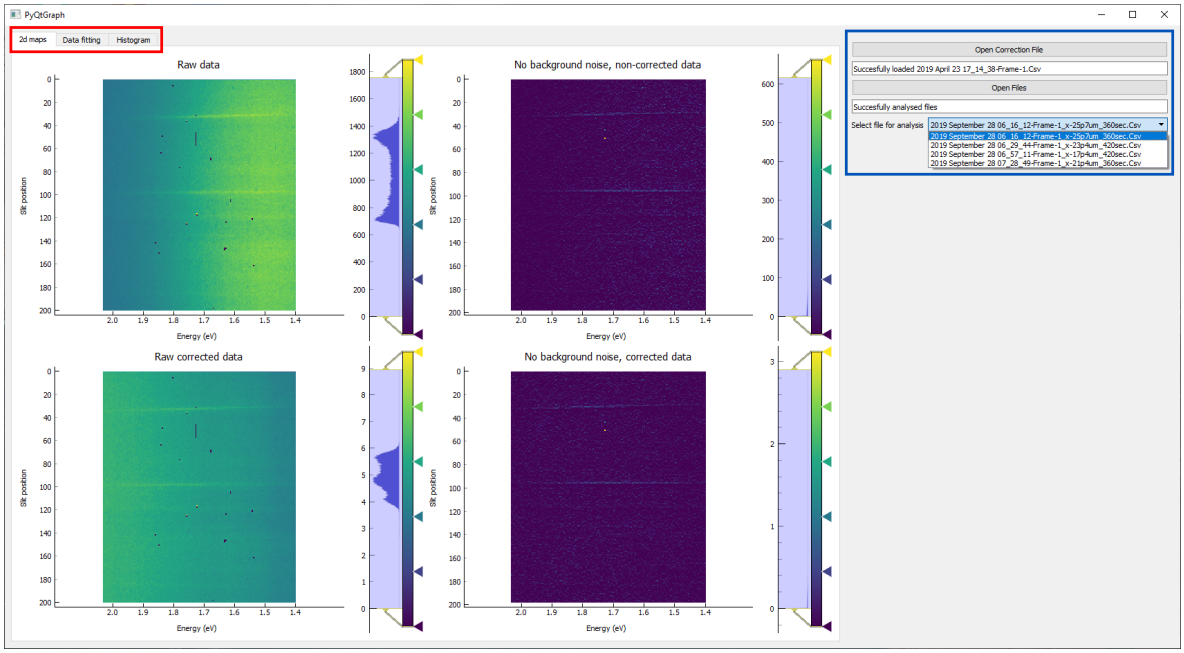

Figure 6: Graphical User Interface as provided by the Python script. The red box in the top left shows the different tab windows, while the blue box on the right shows the User Interface elements. From top to bottom the UI elements in the blue box consist of: a button for uploading the correction file, a status box which gives information about the status of the correction file (i.e. loaded or not loaded), a similar button and status box for the data files and a selection menu for which data-file the user wants to display the graphs for.

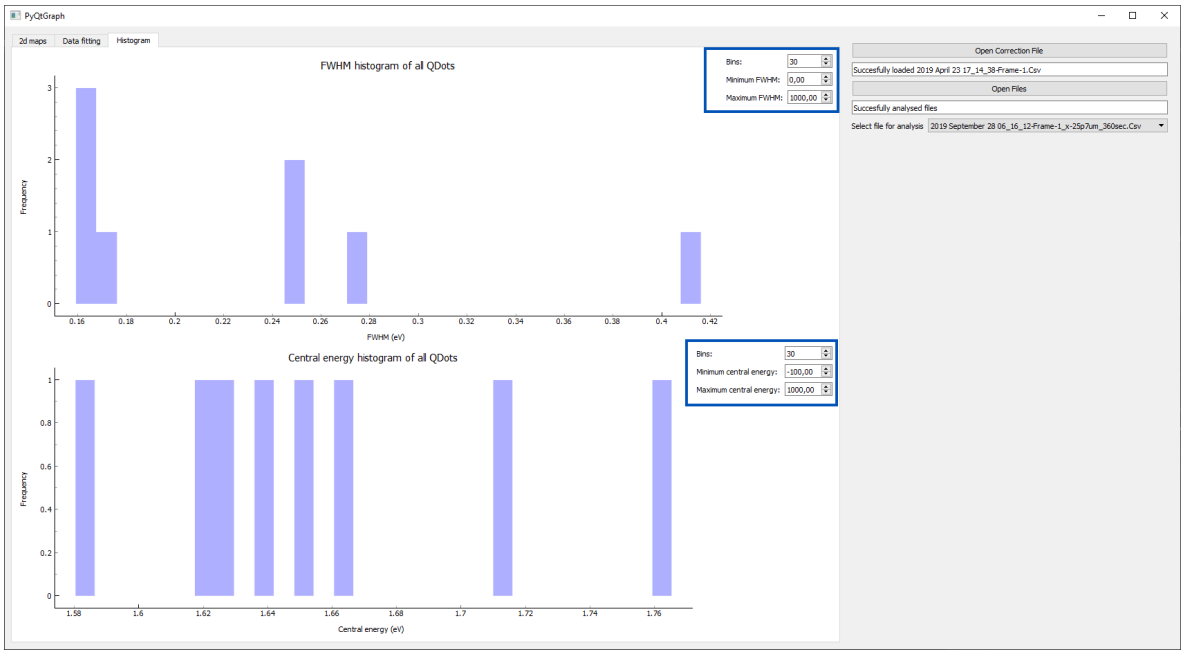

Figure 7: Tabbed window for the histograms in the GUI shown in Figure 6. Shown in the blue boxes is the UI for altering the histograms. The user can change the number of bins as well as changing the lower and upper limit.

References

[1] Chia-Ching Huang, Yingying Tang, Marco van der Laan, Jorik van de Groep, A. Femius Koenderink, and Kateřina Dohnalová. Band-gap tunability in partially amorphous silicon nanoparticles using single-dot correlative microscopy. *ACS Applied Nano Materials*, 0(0):null, 0.

[2] Irshad Ahmad Mir, V. S. Radhakrishanan, Kamla Rawat, Tulika Prasad, and H. B. Bohidar. Bandgap tunable agins based quantum dots for high contrast cell imaging with enhanced photodynamic and antifungal applications. *Scientific Reports*, 8(1):9322, 2018.

[3] Bart van Dam, Clara I. Osorio, Mark A. Hink, Remmert Muller, A. Femius Koenderink, and Katerina Dohnalova. High internal emission efficiency of silicon nanoparticles emitting in the visible range. *ACS Photonics*, 5(6):2129–2136, 2018.

[4] François Gagné, Kenton Leigh, Jennifer Bouldin, and Roger Buchanan. Effects of exposure to semiconductor nanoparticles on aquatic organisms. *Journal of Toxicology*, 2012:397657, 2012.

[5] K Dohnalová, T Gregorkiewicz, and K Kůsová. Silicon quantum dots: surface matters. *Journal of Physics: Condensed Matter*, 26(17):173201, apr 2014.

[6] M. Cahay and Electrochemical Society. *Quantum Confinement VI: Nanostructured Materials and Devices : Proceedings of the International Symposium*. Proceedings (Electrochemical Society). Electrochemical Society, 2001.

[7] Oleg D. Neikov and Nikolay A. Yefimov. Chapter 9 - nanopowders. In Oleg D. Neikov, Stanislav S. Naboychenko, and Nikolay A. Yefimov, editors, *Handbook of Non-Ferrous Metal Powders (Second Edition)*, pages 271 – 311. Elsevier, Oxford, second edition edition, 2019.

[8] Arindam Kole and Partha Chaudhuri. Growth of silicon quantum dots by oxidation of the silicon nanocrystals embedded within silicon carbide matrix. *AIP Advances*, 4(10):107106, 2014.

[9] Encyclopedia of nanoscience and society au - guston, david. page 527, 2010.

[10] M. W. Davidson. Tungsten-halogen incandescent lamps. http://zeiss-campus.magnet.fsu.edu/print/lightsources/tungstenhalogen-print.html.